Temperature Controlled Water/Oil Wettability of a Surface Fabricated by a Block Copolymer: Application as a Dual Water/Oil On–Off Switch

Baolong Xue, Longcheng Gao, Yongping Hou,* Zhiwen Liu, and Lei Jiang*

The manipulation of microfluids has attracted great interest due to its applications in microfluidic devices, water/oil separation, filtration, microreactors, and so on. Many efforts have been made to develop fluidic diode devices with simple operating procedures to achieve the manipulation of fluids. Compared to physical methods, such as pneumatic,[1,2] piezoelectric elements,[3,4] magnetic,[5] centrifugal force,[6] and electrokinetic flow,[7,8] the reversible wettability of an interface controlling liquid flow has many advantages, such as low cost, easy operation, and no additional instruments that occupy the laboratory space.

The wettability of a solid surface is a very important property depending on the chemical composition and the geometric structure of the surface.[9,10] Many smart interfacial materials at the air/solid interface, triggered by light irradiation, electric fields, temperature, pH, solvent treatment, or a combination thereof, have been fabricated.[11–16] For example, the macroscopic motion of liquids on a flat solid surface was manipulated reversibly by photoirradiation of a photoisomerizable monolayer.[17] Poly(*N*-isopropylacrylamide) (PNIPAAm) grafted on the surface of a branched capillary glass tube was used to control water flow based on the thermoresponsive wetting properties.[18] Meanwhile, the wettability at the liquid/solid interface has also been studied. Hierarchical structures of fish scale enable fish to keep their body clean in oil-polluted water. Inspired by these phenomena, a fluoride-free material with a low-adhesive and superoleophobic interface was made by a polyacrylamide hydrogel film.[19] Thermal-responsive reversible switching between superoleophobicity (oil contact angle (OCA) of ≈150°) and oleophobicity (OCA of ≈120°) by PNIPAAm,[20] and electrochemical reversible switching between superoleophobicity and superoleophilicity by polypyrrole,[21] have been realized. It is worth noting that the works above have been focused on the wettability by either water or oil. The control of wettability by both water and oil on one surface (hydrophilicity/hydrophobicity and oleophilicity/oleophobicity) has been barely achieved by changing the outer stimuli. Zhang et al.[22] made pH-sensitive surfaces by grafting a block copolymer (BCP) of poly(2-vinylpyridine)-polydimethylsiloxane, which exhibited both switchable oil wettability by changing the media pH value, and switchable wettability of acidic water at various pH values. However, the surface fabrication and the wettability recovery was complex. Realization of an in situ wettability switch was not achieved, and unexpected contaminants could be introduced. In this article, we provide a simple method to obtain two states of wettability (hydrophilicity/oleophobicity and hydrophobicity/oleophilicity) at different temperatures by direct solution casting of a BCP containing PNIPAAm. By using this wetting surface, a temperature controllable dual water/oil on–off switch was realized. The resultant mesh was open to water and closed to oil below the low critical solution temperature (LCST) of PNIPAAm, and open to oil, closed to water above the LCST.

BCPs, bearing chemically different polymers covalently connected at a single point, can form microphase separated nanostructures. The constructive blocks in the separated nanodomain exhibit their own properties independently, and also affect each other. Thus, BCPs are convenient for the design of smart interfaces. We chose PMMA-*b*-PNIPAAm as the candidate material, in which PNIPAAm is a comprehensively studied thermal-responsive polymer that exhibits an extended hydrophilic chain conformation below its LCST in aqueous solution, and undergoes a phase transition to an insoluble and hydrophobic aggregate above its LCST in air or under water.[20,23] PMMA is hydrophilic with a water CA around 68° on its smooth surface,[24] and oleophilic under water. PMMA has a high glass transition temperature (T_g), and can act as the physical crosslink of PNIPAAm. Therefore, PMMA and PNIPAAm nanodomains self assembled by PMMA-*b*-PNIPAAm exhibit unique wettability properties when the temperature changes, due to their synergistic effect. PMMA-*b*-PNIPAAm was synthesized by atom transfer radical polymerization (ATRP) and a stable BCP film was obtained by direct solution casting.

The BCP with a moderate PNIPAAm volume fraction of 0.55 is supposed to form a lamellar nanostructure. We used in situ atomic force microscopy (AFM) to detect the surface

B. Xue, Prof. L. Gao, Dr. Y. Hou, Prof. L. Jiang
Key Laboratory of Bio-Inspired Smart Interfacial Science and Technology of Ministry of Education
School of Chemistry and Environment
Beihang University
Beijing, 100191, P. R. China
E-mail: lcgao@buaa.edu.cn;
houyongping09@buaa.edu.cn
Dr. Z. Liu
Agilent Technologies, Wang Jing North Road No. 3
Chao Yang District, Beijing, 100102, P. R. China
Prof. L. Jiang
Beijing National Laboratory for Molecular Sciences (BNLMS)
Key Laboratory of Organic Solids
Institute of Chemistry Chinese Academy of Sciences
Beijing, 100190, P. R. China

DOI: 10.1002/adma.201202799

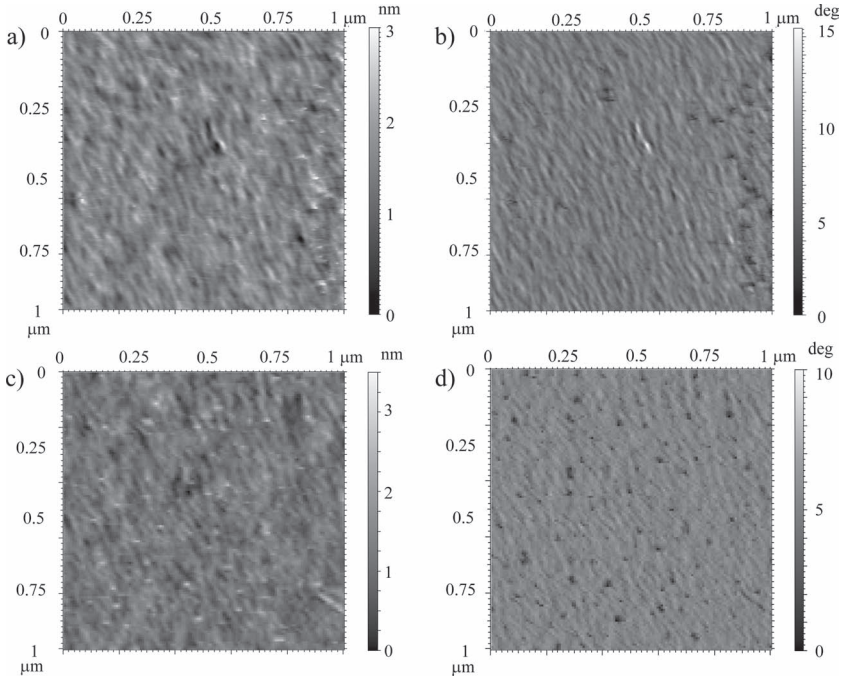

Figure 1. AFM height and phase images of the BCP film under water at 15 °C (a, b) and 30 °C (c, d), indicating that PNIPAAm is swollen below the LCST and shrunken above the LCST.

morphologies and morphology changes under water at different temperatures. **Figure 1** shows the AFM height and phase images at 15 and 30 °C. In both cases, arrays of nanoscopic, lamellar domains of PNIPAAm/PMMA can be seen at the surface of the film. The root-mean-square (RMS) roughness is obtained from the height images at 15 (Figure 1a) and 30 °C (Figure 1c). The RMS roughness at 15 °C is about 0.34 nm, and 0.31 nm at 30 °C. The surface roughness increases by decreasing the temperature. Since the PNIPAAm domains are softer than the PMMA domains, PNIPAAm domains appear brighter in AFM phase images. Compared to the image at 30 °C (Figure 1d), the PNIPAAm domains at 15 °C (Figure 1b) become more obvious and occupy more surface area. These results are related with the temperature sensitivity of PNIPAAm. As shown in **Figure 2**c, at 15 °C (below the LCST), C=O and N–H groups in PNIPAAm form intermolecular hydrogen bonds with water molecules, leading to a hydrated, swollen state of PNIPAAm, which provides PNIPAAm chains on the surface with sufficient mobility to overlay part of the PMMA domains. On the contrary, at 30 °C (above the LCST), C=O and N–H groups form intramolecular hydrogen bonds, leading to a dehydrated, collapsed state. As a result, the PNIPAAm domains shrink compared to that below the LCST. Therefore, not only the PNIPAAm conformation, but also the PNIPAAm domain area changes as the temperature changes. Both of the changes affect the surface wettability.

The CA in air and OCA underwater measurements were conducted to probe the responsive wettability of the BCP surface with different temperatures. The water CAs increase from 42° to 107° and the OCAs (hexane) at the water/BCP interface decrease from 137° to 36° with an increase in temperature from 10 to 40 °C (Figure 2a). This wetting behavior returns to the original state upon cooling, indicating a reversible switching between wetting states of hydrophilicity/oleophobicity and hydrophobicity/oleophilicity. Chen et al.[20] had reported that a thermal-responsive PNIPAAm hydrogel can responsively and reversibly control the wettability and adhesion to oil at a water/solid interface, from a superoleophobic state with low adhesion below the LCST to an oleophobic state with high adhesion above the LCST. The wettability properties were located in the oleophobic area, and oleophilicity cannot be achieved. Here, we chose a BCP of PMMA-*b*-PNIPAAm to achieve two states of wettability (hydrophilicity/oleophobicity and hydrophobicity/oleophilicity) through the cooperation between PNIPAAm and PMMA. The existence of PMMA plays important roles in mediating the wettability. PMMA is oleophilic with an OCA of 35° (Figure S1, Supporting Information). Considering that the wettability of PMMA is less sensitive to temperature, we suppose that the PMMA has a stable oleophilicity. Also, PMMA has a high T_g and PMMA domains remain unchanged ignoring the thermal expansion in the experiment conditions. As seen in Figure 2c, below the LCST, intermolecular hydrogen bonds with water lead to a hydrated, swollen state of PNIPAAm, which provides the surface with a high ratio of water content. Both the PNIPAAm and PMMA are hydrophilic. Therefore, the total surface is hydrophilic and wetted with water. A water-rich surface will effectively block the access of the oil. Consequently, the surface exhibits hydrophilic and oleophobic properties. Above the LCST, intramolecular hydrogen bonds lead to a dehydrated, collapsed state of PNIPAAm. Thus, PNIPAAm is hydrophobic, while PMMA is hydrophilic. PNIPAAm shrinks as the temperature increases, but it still possesses a larger surface area. Therefore, the BCP film is hydrophobic. For oil under water, PMMA is oil-favoured. PNIPAAm with an incomplete degree of dehydration is oil-repelled, just like a PNIPAAm hydrogel, which still possesses a high percentage of water above the LCST.[20] In this system, the BCP self assembles into a lamellar structure. PNIPAAm domains lay in between the hard walls of PMMA on a nanometer scale. Water tends to release from the confined space. The degree of dehydration of PNIPAAm can become quite high with the aid of PMMA in the nanostructure. The nanoPNIPAAm domains become more oleophilic. Therefore, the BCP film is oleophilic. The temperature responsive wettability is related to not only the conformation transition of PNIPAAm, and the apparent PNIPAAm domain area changes, but also the cooperation between PNIPAAm and PMMA.[25] Further experiments of repeatedly cycling at different temperatures show that the as-prepared film undergoes a good transformation between hydrophilicity/oleophobicity and hydrophobicity/oleophilicity (Figure 2b), indicating excellent reproducibility and stability.

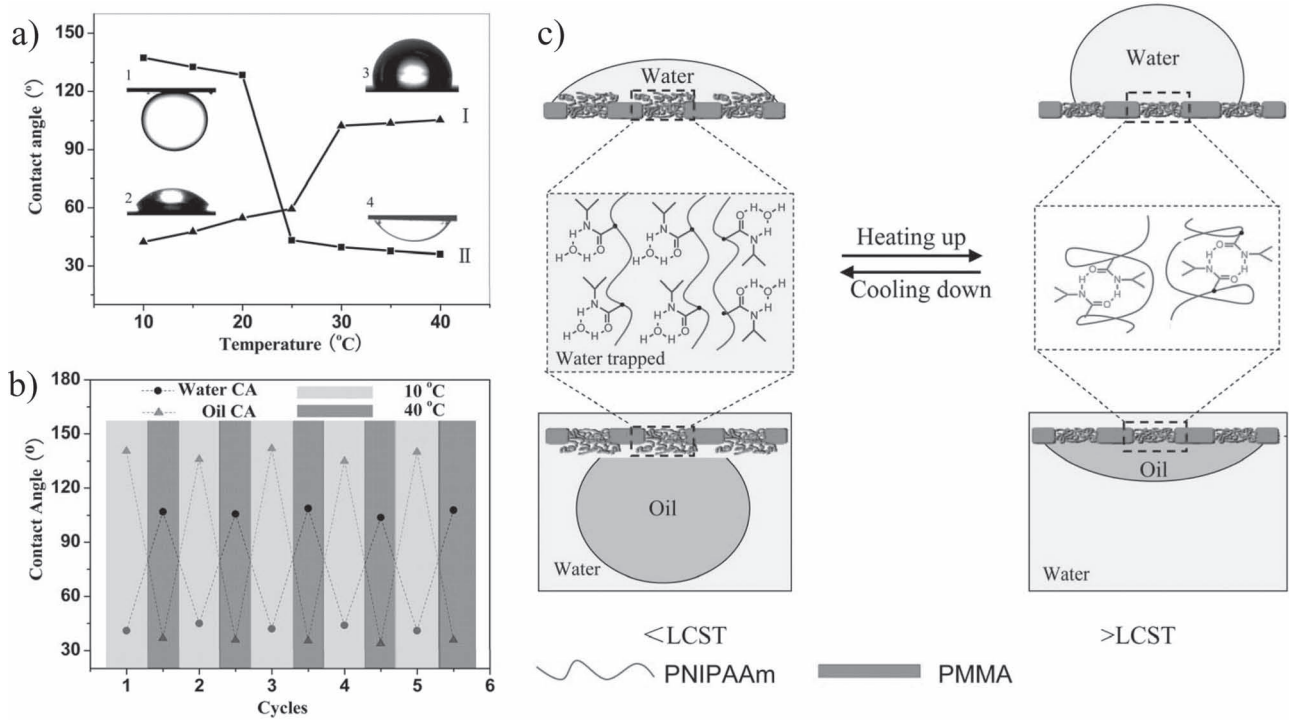

Figure 2. a) Temperature dependences of water and oil CAs for a PMMA-*b*-PNIPAAm film. The water CAs change from 42° to 107° (I) and the OCAs change from 137° to 36° (II) with the temperature increasing from 10 to 40 °C. Inset images (1–4) are the CA/OCA obtained at 10 and 40 °C, respectively. b) Reversible water and oil CA transition of the BCP film at different temperatures (10 °C, < LCST; 40 °C, > LCST), indicating excellent reproducibility and stability. c) Diagram of reversible formation of intermolecular hydrogen bonding between PNIPAAm chains and water molecules below the LCST, which leads to hydrophilicity/oleophobicity, and intramolecular hydrogen bonding between C=O and N–H groups in PNIPAAm chains above the LCST, which leads to hydrophobicity/oleophilicity.

The BCP was solution-cast on a common industrial steel mesh. Compared to the polymer-grafting method, this method has great advantages of low cost, fast preparation, independence of substrate, arbitrary size, and so on. Surface geometrical structures play an important role in the wettability of a thin film.[26] According to Wenzel's theory,[27] the surface roughness enhances both the hydrophilicity (oleophobicity) of a hydrophilic (oleophobic) film and the hydrophobicity (oleophilicity) of a hydrophobic (oleophilic) film. In order to augment the responsive wettability of the film, we used the water droplet templating method to increase the surface roughness.[28] As shown in Figure S2 (Supporting Information), significant differences are observed between the initial steel mesh and the BCP-coated steel mesh. The scanning electron microscopy (SEM) images (Figure S2a,b) show that the initial mesh is knitted by metal wires and the average diameter is about 85 μm. After coating with BCP (Figure S2c), the average diameter increases to 90 μm. Moreover, the highly magnified images (Figure S2d) show that micropore structures are formed on the surface because of the condensed water effect as expected.[28]

Figure 3 shows the spreading and permeating behaviours of a pure water and oil droplet on the BCP-coated mesh at different temperatures. As shown in Figure 3a, at 15 °C (below the LCST of PNIPAAm), water spreads quickly on the BCP-covered steel mesh and permeates through freely (≈5 s), showing highly hydrophilic properties. On the contrary, a hexane droplet underwater cannot permeate through the mesh, and sticks to the mesh surface (Figure 3b). On the other hand, at 30 °C (above the LCST of PNIPAAm), the hexane droplet spreads quickly on the BCP-coated mesh and penetrates through quickly (≈1 s) (Figure 3d), while a water droplet stays still on the surface and cannot go through the mesh during the measurement (Figure 3c). The observations above are in accordance with a wettability change. Therefore, a temperature controllable dual water/oil on–off switch is realized based on the temperature-controlled wettability.

Furthermore, the on–off switch also worked in a water/oil mixture and on an amplified scale. The experiment procedure was performed as shown in **Figure 4**. A piece of BCP-coated mesh was used to seal the bottleneck of a glass tube. The tube was then put into the water and oil (coloured with iodine) mixture with magnetic stirring. Water penetrates the mesh and is collected in the bottle at 15 °C (Figure 4d), while oil can be collected at 30 °C (Figure 4e). Other oils such as petroleum ether and *n*-heptane exhibit similar behaviors (Figure S3, Supporting Information). These results are in accordance with the results from pure water and oil. It is obvious that a highly effective temperature-controlled dual water/oil on–off switch on a macroscale is achieved using the BCP-coated mesh. In addition, after repeating the water/oil separation experiments for more than 10 times at 15 and 30 °C, the mesh still retains a good separation

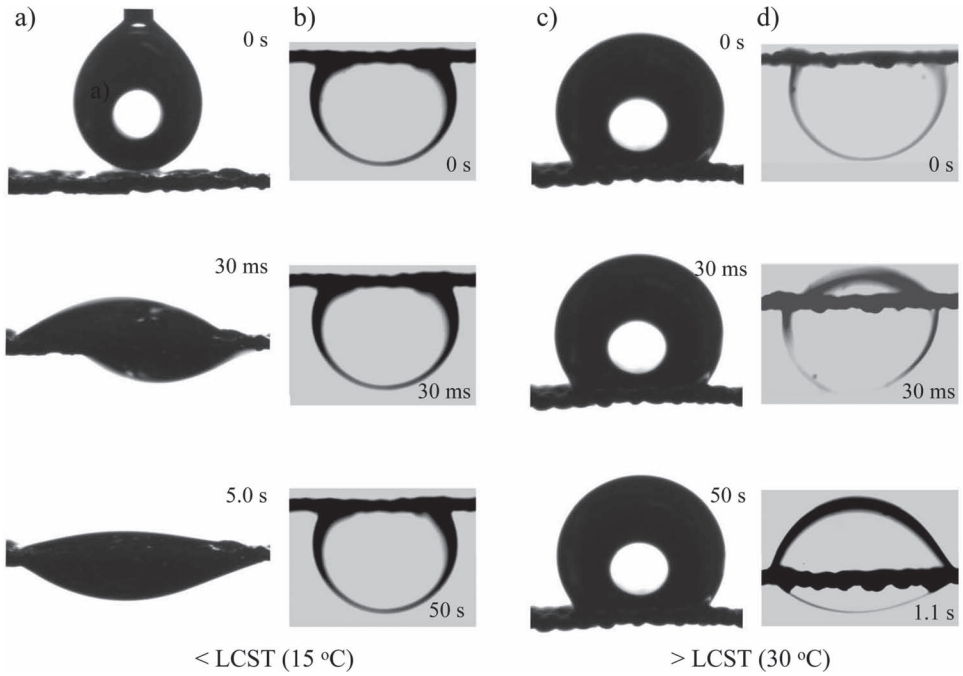

Figure 3. Temperature-controlled pure water/oil on-off switch based on a BCP-coated mesh. Below the LCST, a water droplet permeated through the mesh (a) and an oil droplet could not (b). Above the LCST, a water droplet could not permeate through the mesh (c), while a oil droplet could (d).

ability, indicating that the adhesion strength between the BCP film and the substrate and the solvent-resistance of the mesh is good.

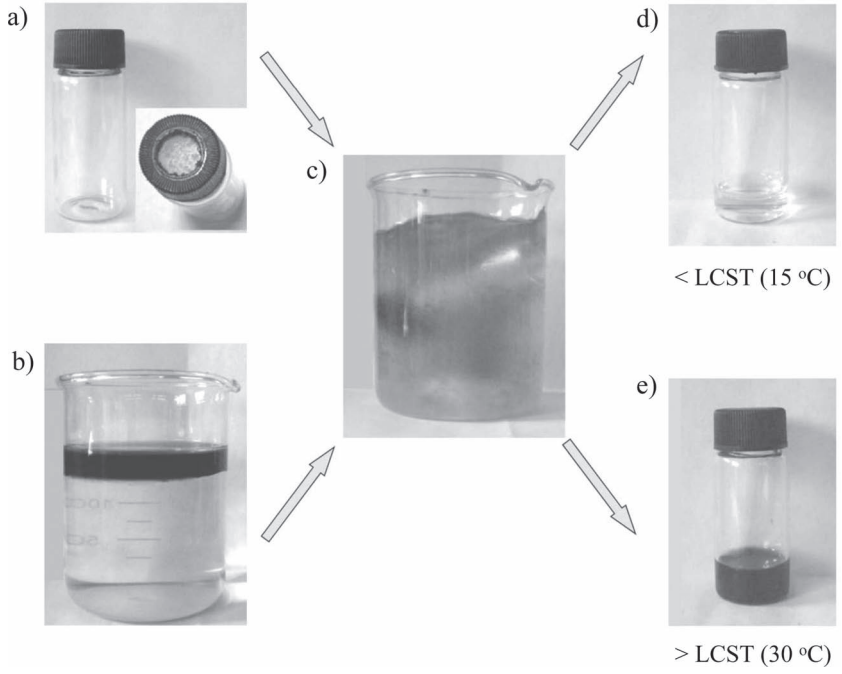

Figure 4. Temperature-controlled mixed water/oil on–off switch based on a BCP-coated mesh. A piece of BCP-coated mesh was used to seal a glass bottle cap (a). Sufficient water and oil (oil was colored with iodine) mixture was put into a beaker (b). A glass bottle was put into the water and oil mixture at different temperatures with stirring (c). Water was collected below the LCST (d) and oil was collected above the LCST (e).

The unique temperature-controlled dual water/oil on–off switch corresponds to the temperature controlled wettability. Consequently, the temperature controlled wettability corresponds to the discontinuous conformational change of the PNIPAAm chain around the LCST, as well as the self assembled structure and cooperation between PNIPAAm and PMMA. Below the LCST, the BCP-coated mesh exhibits states of hydrophilicity and oleophobicity. Water can permeate through the BCP-coated mesh, while oil cannot. Above the LCST, the mesh exhibits states of hydrophobicity and oleophilicity. An oil droplet spreads quickly on the BCP-coated mesh and penetrates through quickly. Meanwhile, a water droplet stays still on the surface and cannot go through the mesh. Therefore, a dual water/oil on–off switch is achieved. Further research is still in progress.

In conclusion, we fabricated a connection between chemical structure and properties. Symmetric PMMA-*b*-PNIPAAm self assembled into lamellar nanostructures. A discontinuous conformational change of the PNIPAAm chain and the resultant surface roughness change around the LCST, as well as cooperation between PNIPAAm and PMMA domains, imparted the BCP film with reversible switching between wettability states of hydrophilicity/oleophobicity and hydrophobicity/oleophilicity at different

temperatures. By direct casting of the BCP solution onto a common industrial steel mesh, a temperature controlled dual water/oil on–off switch was achieved. Water could permeate through the BCP-coated mesh, and oil could not below the LCST; however, oil could and water could not above the LCST. This work offers promising applications of the film in the controllable separation of water and oil mixtures, in filtration and microreactors, lab-on-chip devices, micro/nanofluidic devices, and so on.

Experimental Section

Materials: The stainless steel meshes with pore sizes of 120 to 140 μm were purchased from Daoxu Company in China. Hexane was obtained from Beijing Chemical Co. (Chemical purity). All the chemical reagents were used as received without any purification. The PMMA-*b*-PNIPAAM BCP was synthesized by sequential ATRP as described elsewhere. The number-average molecular weight (M_n) of the PMMA macroinitiator was 21 000 and the polydispersity index (PDI) was 1.17. The M_n of PMMA-*b*-PNIPAAm BCP was 46 400 and the PDI was 1.16. The calculated weight percent of PNIPAAM was 59.3% determined by ^{1}H NMR spectroscopy. The volume fraction of PNIPAAm was 0.55, as the known density of PNIPAAm and PMMA is 1.39 and 1.18 g cm^3, respectively.[29]

Preparation of the BCP Film: A flat BCP film was prepared by solution casting a 1.0 g mL^{-1} BCP solution in tetrahydrofuran (THF) on a glass slide (2 cm × 2 cm) in a semi-closed box avoiding humidity. After the solvent slowly evaporated over 1 day, the glass slide was put into an oven at 50 °C for another day, and then under vacuum to remove the residual solvent. A BCP-coated film was made, in a simple way, by solution casting a 1.0 g mL^{-1} BCP solution in THF onto a stainless steel mesh drop by drop. As the THF evaporated under the given conditions (temperature: 25 °C, humidity: 75%), the BCP formed a thin layer around the steel wire.

Characterization: The structures of metal mesh and BCP-coated metal mesh were observed by SEM (Quanta FEG 250, FEI, America) at 10 kV with gold plating. Water and oil CAs were measured by the optical contact angle meter system (OCA40Micro, Dataphysics Instruments GmbH, Germany). A 2.0 μL aliquot of deionized water or oil was dropped onto the samples and the static CA was determined by the average of at least five measurements taken at different positions on each sample. The whole permeating process of pure water/oil was recorded by the optical microscopy and CCD components of the OCA40 system. In situ AFM measurements were carried out under water at 15 and 30 °C. AFM experiments were performed using an Agilent AFM series 5500 (Agilent Technologies). Imaging was carried out in the AAC mode. The used cantilevers (Nanosensor) had frequencies within 204–497 kHz and force constant values of 10–130 N m^{-1}. The root-mean-square (RMS) roughness was evaluated by analyzing the 2D height images with the Picoimage software.

Supporting Information

Supporting Information is available from the Wiley Online Library or from the author.

Acknowledgements

This work is supported by National Natural Science Foundation of China (21204002, 51203006), National Key Basic Research Program of Chian (213CB933000), Specialized Research Fund for the Doctoral Program of Higher Education (20111102120049, 20111102120050) and the Fundamental Research Funds for the Central Universities.

Received: July 11, 2012
Published online: October 17, 2012

[1] D. C. Leslie, C. J. Easley, E. Seker, J. M. Karlinsey, M. Utz, M. R. Begley, J. P. Landers, *Nat. Phys.* **2009**, *5*, 231.
[2] M. A. Unger, H.-P. Chou, T. Thorsen, A. Scherer, S. R. Quake, *Science* **2000**, *288*, 113.
[3] I. D. Johnston, M. C. Tracey, J. B. Davis, C. K. L. Tan, *Lab Chip* **2005**, *5*, 318.
[4] A. Bransky, N. Korin, M. Khoury, S. Levenberg, *Lab Chip* **2009**, *9*, 516.
[5] S. Bleil, D. W. M. Marr, C. Bechinger, *Appl. Phys. Lett.* **2006**, *88*, 263515.
[6] D. C. Duffy, H. L. Gillis, J. Lin, N. F. Sheppard, G. J. Kellogg, *Anal. Chem.* **1999**, *71*, 4669.
[7] J. W. Hong, S. R. Quake, *Nat. Biotechnol.* **2003**, *21*, 1179.
[8] J. Yang, D. Y. Kwok, *Langmuir* **2003**, *19*, 1047.
[9] L. Feng, Z. Zhang, Z. Mai, Y. Ma, B. Liu, L. Jiang, D. Zhu, *Angew. Chem. Int. Ed.* **2004**, *43*, 2012.
[10] C. Wang, T. Yao, J. Wu, C. Ma, Z. Fan, Z. Wang, Y. Cheng, Q. Lin, B. Yang, *ACS Appl. Mater. Interfaces* **2009**, *1*, 2613.
[11] G. M. Whitesides, P. E. Laibinis, *Langmuir* **1990**, *6*, 87.
[12] C. D. Bain, G. M. Whitesides, *Angew. Chem. Int. Ed.* **1989**, *28*, 506.
[13] S. Wang, X. Feng, J. Yao, L. Jiang, *Angew. Chem. Int. Ed.* **2006**, *45*, 1264.
[14] H. Bai, X. Tian, Y. Zheng, J. Ju, Y. Zhao, L. Jiang, *Adv. Mater.* **2010**, *22*, 5521.
[15] G. Möller, M. Harke, H. Motschmann, D. Prescher, *Langmuir* **1998**, *14*, 4955.
[16] L. M. Siewierski, W. J. Brittain, S. Petrash, M. D. Foster, *Langmuir* **1996**, *12*, 5838.
[17] K. Ichimura, S.-K. Oh, M. Nakagawa, *Science* **2000**, *288*, 1624.
[18] T. Saitoh, Y. Suzuki, M. Hiraide, *Anal. Sci.* **2002**, *18*, 203.
[19] M. Liu, S. Wang, Z. Wei, Y. Song, L. Jiang, *Adv. Mater.* **2009**, *21*, 665.
[20] L. Chen, M. Liu, L. Lin, T. Zhang, J. Ma, Y. Song, L. Jiang, *Soft Matter* **2010**, *6*, 2708.
[21] M. Liu, X. Liu, C. Ding, Z. Wei, Y. Zhu, L. Jiang, *Soft Matter* **2011**, *7*, 4163.
[22] L. Zhang, Z. Zhang, P. Wang, *NPG Asia Mater.* **2012**, *4*, e8.
[23] T. Sun, G. Wang, L. Feng, B. Liu, Y. Ma, L. Jiang, D. Zhu, *Angew. Chem. Int. Ed.* **2004**, *43*, 357.
[24] Y. Ma, X. Cao, X. Feng, Y. Ma, H. Zou, *Polymer* **2007**, *48*, 7455.
[25] T. Sun, W. Song, L. Jiang, *Chem. Commun.* **2005**, 1723.
[26] Y. Hou, Y. Chen, Y. Xue, Y. Zheng, L. Jiang, *Langmuir* **2012**, *28*, 4737.
[27] R. N. Wenzel, *J. Phys. Colloid Chem.* **1948**, *53*, 1466.
[28] M. Srinivasarao, D. Collings, A. Philips, S. Patel, *Science* **2001**, *292*, 79.
[29] *Polymer Data Handbook* (Ed: E. J. Mark), Oxford University Press, New York **1999**.